

Superhydrophobic surfaces cannot reduce ice adhesion

Jing Chen, Jie Liu, Min He, Kaiyong Li, Dapeng Cui, Qiaolan Zhang, Xiping Zeng, Yifan Zhang, Jianjun Wang, and Yanlin Song

Citation: [Applied Physics Letters](#) **101**, 111603 (2012); doi: 10.1063/1.4752436

View online: <http://dx.doi.org/10.1063/1.4752436>

View Table of Contents: <http://scitation.aip.org/content/aip/journal/apl/101/11?ver=pdfcov>

Published by the [AIP Publishing](#)

Articles you may be interested in

[Does surface roughness amplify wetting?](#)

J. Chem. Phys. **141**, 184703 (2014); 10.1063/1.4901128

[Wetting of soap bubbles on hydrophilic, hydrophobic, and superhydrophobic surfaces](#)

Appl. Phys. Lett. **102**, 254103 (2013); 10.1063/1.4812710

[Switchable electrowetting of droplets on dual-scale structured surfaces](#)

J. Vac. Sci. Technol. B **30**, 06F801 (2012); 10.1116/1.4764092

[Frost formation and ice adhesion on superhydrophobic surfaces](#)

Appl. Phys. Lett. **97**, 234102 (2010); 10.1063/1.3524513

[Surface texture and wetting stability of polydimethylsiloxane coated with aluminum oxide at low temperature by atomic layer deposition](#)

J. Vac. Sci. Technol. A **28**, 1330 (2010); 10.1116/1.3488604

An advertisement for Keysight B2980A Series Picoammeters/Electrometers. The ad features a red and white color scheme. On the left, text reads 'Confidently measure down to 0.01 fA and up to 10 PΩ' and 'Keysight B2980A Series Picoammeters/Electrometers'. Below this is a red button with the text 'View video demo'. On the right, there is an image of the Keysight B2980A device and the Keysight Technologies logo.

Superhydrophobic surfaces cannot reduce ice adhesion

Jing Chen,^{1,2} Jie Liu,^{1,2} Min He,^{1,2} Kaiyong Li,^{1,2} Dapeng Cui,^{1,2} Qiaolan Zhang,^{1,2} Xiping Zeng,^{1,2} Yifan Zhang,^{1,2} Jianjun Wang,^{1,a)} and Yanlin Song¹

¹Beijing National Laboratory for Molecular Sciences (BNLMS), Institute of Chemistry, Chinese Academy of Sciences, Beijing 100190, People's Republic of China

²Graduate University of Chinese Academy of Sciences, Beijing 100049, People's Republic of China

(Received 18 June 2012; accepted 28 August 2012; published online 13 September 2012)

Understanding the mechanism of ice adhesion on surfaces is crucial for anti-icing surfaces, and it is not clear if superhydrophobic surfaces could reduce ice adhesion. Here, we investigate ice adhesion on model surfaces with different wettabilities. The results show that the superhydrophobic surface cannot reduce the ice adhesion, and the ice adhesion strength on the superhydrophilic surface and the superhydrophobic one is almost the same. This can be rationalized by the mechanical interlocking between the ice and the surface texture. Moreover, we find that the ice adhesion strength increases linearly with the area fraction of air in contact with liquid. © 2012 American Institute of Physics. [<http://dx.doi.org/10.1063/1.4752436>]

Accumulated ice on exposed surfaces leads to operational difficulties and high maintenance efforts for power transmission lines, antennas, aircrafts, ships, and ground transportation vehicles.^{1–6} Over the last several decades, a large number of investigations have been carried out focusing on anti-icing surfaces via preventing ice formation or reducing ice adhesion.^{7–16} Ice formation is inevitable when the temperature is lowered sufficiently.¹⁷ Therefore, ideal anti-icing surfaces would be that the ice adhesion on these surfaces is so small that ice formed on them could be shed off merely due to its own weight or a natural wind action. Thus reducing the ice adhesion on surfaces is the key for fighting against icing on surfaces, which requires a thorough understanding of the mechanism of ice adhesion on surfaces. Recently, it has been reported that superhydrophobic surfaces could substantially reduce the ice adhesion.^{18–20} Some authors even correlated the contact angle hysteresis with the ice adhesion.²¹ But this statement was questioned, for example, Varanasi *et al.*¹⁷ reported that the frost formation inside the textures of superhydrophobic surfaces could increase the ice adhesion and thus compromised their effectiveness in reducing the ice adhesion and Varanasi's argument was supported by other research groups, who reported that the ice adhesion increased with the surface roughness.^{22,23}

To address this controversy, we investigated the ice adhesion on a series of model surfaces with distinct wettabilities. We found that superhydrophobic surfaces could not reduce the ice adhesion and the ice adhesion on superhydrophobic surfaces was almost the same as that on the superhydrophilic surfaces. This could be explained when the mechanical interlocking between the ice and the surface texture was considered. Moreover, a correlation between the ice adhesion and the area fraction of air in contact with liquid was established. These studies provide valuable insights into the mechanisms of the ice adhesion on surfaces and will be beneficial for the rational design of anti-icing surfaces.

Thirteen silicon wafer surfaces with wettability ranging from superhydrophilic to superhydrophobic were designed and fabricated to study the influence of the surface morphology and chemistry on the ice adhesion. The textured silicon wafer surfaces with groove and pore arrays (two microgrooved surfaces with distinct wettabilities, i.e., superhydrophilic and superhydrophobic, have the same morphology but different surface chemistry. Four hydrophilic pore array surfaces and four hydrophobic pore array surfaces have the same pore size, but different distance between neighboring pores and surface chemistry.) were prepared by a photolithographic process and detailed information of tested sample surfaces are summarized in Table I.

The setup for measuring the ice adhesion is similar to the one used by Varanasi *et al.*²⁴ as sketched in Figure S1. In detail, the setup consists of an XY motion stage, a force transducer (Imada ZP-500N), a home built cooling stage, and water-filled cuvettes that are frozen onto the tested surfaces. Then the cooling stage with the cuvettes atop of it was placed in a closed box, which was purged with nitrogen gas to minimize the frost formation outside of the cuvettes. The probe of the force transducer was propelled perpendicularly to the ice column at a speed of 0.5 mm/s, and the shear stress required to detach each ice column from the surface was obtained. The peak force was converted into the ice adhesion strength via dividing it by the ice cross-sectional area (see the supplementary material³⁰). Our experiments showed that the ice adhesion remained constant when the surface temperature changed from -10 to -20 °C or the probe speed varied from 0.5 to 1.5 mm/s (see Figure S2), which agreed with the data obtained by Varanasi *et al.*²⁴ Therefore, we investigated the ice adhesion strength at surface temperature of -15 °C and a probe speed of 0.5 mm/s. The measurement was carried out after the water in the cuvette was kept at -15 °C for 5 h, which ensured that water froze completely. The ice adhesion strength for each surface was averaged over 8 tests.

Figure 1 shows the ice adhesion strengths to four surfaces (superhydrophilic, hydrophilic, hydrophobic, and superhydrophobic). The ice adhesion strength on the superhydrophilic surface is the highest, i.e., 913 ± 138 kPa. This could be

^{a)} Author to whom correspondence should be addressed. Electronic mail: wangj220@iccas.ac.cn.

TABLE I. Geometrical and static contact angle of representative surfaces.

Sample	Features (μm)			Static contact angle ($^\circ$)
	Width	Depth	Spacing	
Groove array (superhydrophilic)	5	5	5	4.2 ± 1.0
Silicon surface (hydrophilic)		Smooth		8.5 ± 1.2
Silicon surface (hydrophobic)		Smooth		114.4 ± 0.5
Groove array (superhydrophobic)	5	5	5	154.0 ± 1.8
Pore array a (hydrophilic)	5	5	40	24.8 ± 0.8
Pore array b (hydrophilic)	5	5	20	23.8 ± 1.3
Pore array c (hydrophilic)	5	5	10	18.8 ± 1.0
Pore array d (hydrophilic)	5	5	5	15.1 ± 0.5
Pore array a (hydrophobic)	5	5	40	111.7 ± 1.6
Pore array b (hydrophobic)	5	5	20	115.3 ± 2.4
Pore array c (hydrophobic)	5	5	10	118.6 ± 2.7
Pore array d (hydrophobic)	5	5	5	128.0 ± 1.3
Silicon surface as-received	Smooth			75.4 ± 1.0

explained by considering that liquid water on this surface is at the Wenzel state, i.e., the liquid water impregnate completely into the surface texture. When the liquid water solidified into ice, mechanical interlocking formed between the ice and the surface texture. The ice adhesion strength on the flat hydrophilic surface is 202 ± 34 kPa, which is 4.5 times lower than that on the superhydrophilic surface. This could be attributed to the smoothness of the hydrophilic silicon wafer, on which almost no mechanical interlocking formed. The ice adhesion strength on the hydrophobic surface is even lower than that of the smooth hydrophilic surface, i.e., 77 ± 16 kPa. This can be rationalized by hydrogen bonds formed between the surface and the ice, which was believed to be an important factor controlling the strength of ice adhesion.²⁵ A large number of hydrogen bonds can be formed on the hydrophilic silicon wafer surface due to the large number of hydroxyl groups on it. On the contrary, there is almost no hydroxyl group on the surface when the silicon wafer surface was modified with (heptadecafluoro-1,1,2,2-tetradecyl)-trimethoxysilane, thus hydrogen bonds could not form between this surface and the ice. To confirm this argument, the ice adhesion strength on as-received flat silicon wafer (CA (water contact angle) = $75.4^\circ \pm 1.0^\circ$) was measured, which had a value larger

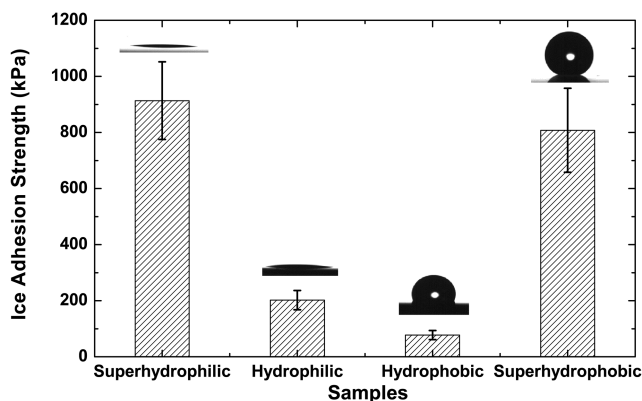


FIG. 1. Average ice adhesion strengths on four different silicon wafer surfaces (superhydrophilic to superhydrophobic) measured at -15°C with a probe speed of 0.5 mm/s. Insets are the profiles of water droplets on the corresponding surfaces.

than hydrophobic silicon wafer surface (CA = $114.4^\circ \pm 0.5^\circ$) but smaller than hydrophilic one (CA = $8.5^\circ \pm 1.2^\circ$), resulting from the difference in the hydroxyl group density on these surfaces. (see Figure S3).

Surprisingly, the ice adhesion strength on superhydrophobic surface is 807 ± 149 kPa, which is almost the same as that on the superhydrophilic surface. For superhydrophobic surfaces, liquid water sits atop of the surface texture at the room temperature, in other words, the liquid water is at the Cassie state. The air trapped inside the surface texture beneath the liquid water is in thermodynamically equilibrium with the liquid water. When the temperature is lowered, water molecules adsorb at the wall of the surface texture, which makes the surfaces more hydrophilic. At the same time, condensation occurs inside the surface texture when the temperature is lowered.^{26–28} Then the liquid water is not at the Cassie state anymore, i.e., it penetrates partially or even completely into the surface texture. When the liquid water freezes, the ice and the surface texture are mechanically interlocked and this results in the increased ice adhesion strength.

To further elucidate the effects of the surface morphology and chemistry on the ice adhesion, a series of hydrophilic and hydrophobic silicon wafer surfaces composed of pore arrays were fabricated and the ice adhesion strengths on these surfaces were measured. The pore array surfaces consist of periodic pores that are $5 \mu\text{m}$ in width and depth, and the space between the neighboring pores varies from $5 \mu\text{m}$ to $40 \mu\text{m}$ (showed in the insets of Figure 2). Here, we define ϕ as the area fraction of air in contact with liquid at the liquid substrate interface

$$\phi = a^2/(a+b)^2, \quad (1)$$

where a is the width of the pore and b is the space between two neighboring pores. The corresponding ϕ is 0.25, 0.11, 0.06, and 0.04 on the textured silicon surfaces with the spacing 5, 10, 20, and $40 \mu\text{m}$, respectively. Hydrophilic and

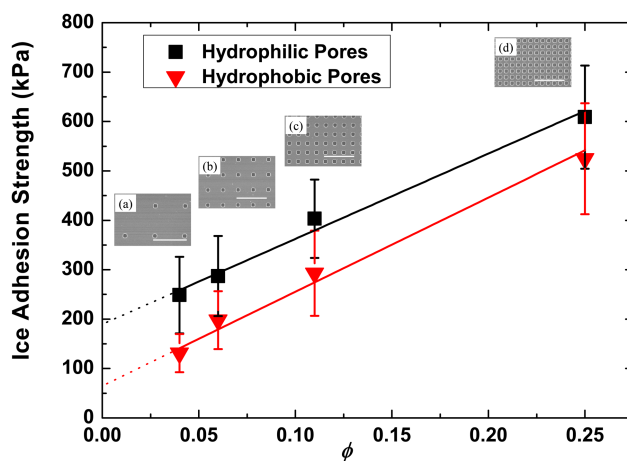


FIG. 2. Plots of the measured ice adhesion strength on the textured surfaces as a function of ϕ (area fraction of air in contact with liquid). The ice adhesion measurements on textured surfaces were measured at -15°C with a probe speed of 0.5 mm/s. The ice adhesion strength increases with the ϕ value. The solid lines show the linear fit to the data with coefficient $R^2 = 0.98$ and $R^2 = 0.97$ for hydrophilic and hydrophobic surfaces, respectively. The Y-intercepts (extrapolated using a dashed line) denote the adhesive strength of ice on the smooth surfaces. Insets [(a)-(d)] are top-view SEM images of pore array surfaces with different spacing (40, 20, 10, and $5 \mu\text{m}$, respectively) between neighboring pores. Scale bar is $50 \mu\text{m}$.

hydrophobic sample surfaces composed of pore array were prepared by treating textured silicon surfaces with piranha solution and (heptadecafluoro-1,1,2,2-tetradecyl)-trimethoxysilane, respectively. The static water contact angles for hydrophilic pore array surfaces are ranging from 15° to 25°, and for hydrophobic surfaces, the static water contact angles are in the range of 111° to 128°.

Figure 2 plots the ice adhesion strength of the textured surfaces as a function of the area fraction of air in contact with liquid, which clearly reveals a strong linear function with correlation coefficient of $R^2=0.98$ and $R^2=0.97$ for hydrophilic and hydrophobic surfaces, respectively. Then the adhesive strength between the ice and the substrates can be extrapolated from the fitting lines when the area fraction of air in contact with liquid approaches zero. It equals 186 kPa for the hydrophilic surface and 63 kPa for hydrophobic surface. These extrapolated values are close to the experimental values shown in Figure 1, which are 202 kPa and 77 kPa for the flat hydrophilic and hydrophobic surfaces, respectively. Similarly, the cohesive strength can be calculated when the area fraction of air in contact with liquid equals one, which is 1916 kPa and 1970 kPa for hydrophilic and hydrophobic surface, respectively. A similar result was reported by Jellinek for snow-ice frozen to polished steel plates, in which the cohesive strength was about 1600 kPa.²⁹ Removal of the ice from the textured surfaces need to overcome the adhesive strength between the ice and substrate as well as the cohesive strength due to the mechanical interlocking as schematically shown in Figure 3.

More cohesive failure is required when the area fraction of air in contact with liquid increases and this leads to a larger ice adhesion strength because the cohesive strength is much bigger than the adhesive strength. So the ice adhesion strength can be expressed as following:

$$F = F_{coh} \times \phi + F_{adh} \times (1 - \phi). \quad (2)$$

After rearranging, the equation becomes

$$F = F_{adh} + \phi \times (F_{coh} - F_{adh}), \quad (3)$$

where F is the ice adhesion strength, F_{coh} is the cohesive strength, and F_{adh} is the adhesive strength. Since there is no mechanical interlocking effect on the smooth surface, the ice adhesion strength on smooth silicon substrates is much smaller than that of textured surfaces. Equation (3) shows that the surface chemistry difference results in the slight slope difference of two fitted lines in Figure 2, because F_{coh} is one order of magnitude larger than F_{adh} . Therefore, the ice

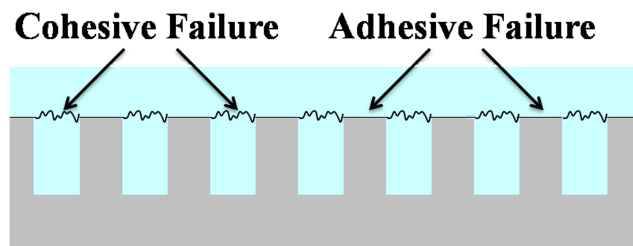


FIG. 3. Proposed model for the ice adhesion failure mechanism on the patterned substrate.

adhesion strength on the superhydrophobic surface and superhydrophilic surface is almost the same and much bigger than that of the smooth surfaces.

In conclusion, we systematically investigated the influence of surface morphology and chemistry on the ice adhesion strength. Textured surfaces show higher ice adhesion strength than smooth surfaces, resulting from the mechanical interlocking formed between the ice and the surface texture. These results show that superhydrophobic surfaces cannot reduce ice adhesion. Furthermore, a correlation between the ice adhesion strength and the area fraction of air in contact with liquid was established. The ice adhesion strength increases linearly with the increase of the area fraction of air in contact with liquid. This finding deepens our understanding of the mechanism of ice adhesion on surfaces and provides guidance for the design of anti-icing surfaces.

The authors are grateful for the financial support from the Chinese National Nature Science Foundation (Grant Nos. 51173196, 21004068) and the 973 Program (2012CB933800).

- ¹V. K. Croutch and R. A. Hartley, *J. Coat. Technol.* **64**, 41 (1992).
- ²M. R. Kasaai and M. Farzaneh, in *Proceedings of OMAE04: 23rd International Conference on Offshore Mechanics and Arctic Engineering*, Vancouver, British Columbia, Canada (2004), Vol. 25, pp. 927–932.
- ³R. Menini and M. Farzaneh, *Surf. Coat. Technol.* **203**, 1941 (2009).
- ⁴S. Frankenstein and A. M. Tuthill, *J. Cold Reg. Eng.* **16**, 83 (2002).
- ⁵M. G. Ferrick, N. D. Mulherin, B. A. Coutermarsh, G. D. Durell, L. A. Curtis, T. L. St. Clair, E. S. Weiser, R. J. Cano, T. M. Smith, C. G. Stevenson, and E. C. Martinez, *J. Adhes. Sci. Technol.* **26**, 473 (2012).
- ⁶R. J. Cano, E. S. Weiser, T. M. Smith, S. Trigwell, L. A. Curtis, and D. Drewry, *J. Adhes. Sci. Technol.* **26**, 621 (2012).
- ⁷L. Cao, A. K. Jones, V. K. Sikka, J. Wu, and D. Gao, *Langmuir* **25**, 12444 (2009).
- ⁸P. Tourkine, M. Le Merrer, and D. Quéré, *Langmuir* **25**, 7214 (2009).
- ⁹L. Mishchenko, B. Hatton, V. Bahadur, J. A. Taylor, T. Krupenkin, and J. Aizenberg, *ACS Nano* **4**, 7699 (2010).
- ¹⁰A. J. Meuler, G. H. McKinley, and R. E. Cohen, *ACS Nano* **4**, 7048 (2010).
- ¹¹M. He, J. Wang, H. Li, and Y. Song, *Soft Matter* **7**, 3993 (2011).
- ¹²P. Guo, Y. Zheng, M. Wen, C. Song, Y. Lin, and L. Jiang, *Adv. Mater.* **24**, 2642 (2012).
- ¹³J. Xiao and S. Chaudhuri, *Langmuir* **28**, 4434 (2012).
- ¹⁴A. Dotan, H. Dodiuk, C. Laforte, and S. Kenig, *J. Adhes. Sci. Technol.* **23**, 1907 (2009).
- ¹⁵D. K. Sarkar and M. Farzaneh, *J. Adhes. Sci. Technol.* **23**, 1215 (2009).
- ¹⁶J. M. Sayward, “Seeking low ice adhesion,” Special Report 79-11, U.S. Army Cold Regions Research and Engineering Laboratory, Hanover, NH, 1979.
- ¹⁷K. K. Varanasi, T. Deng, J. D. Smith, M. Hsu, and N. Bhate, *Appl. Phys. Lett.* **97**, 234102 (2010).
- ¹⁸S. A. Kulinich and M. Farzaneh, *Appl. Surf. Sci.* **255**, 8153 (2009).
- ¹⁹S. A. Kulinich and M. Farzaneh, *Cold Regions Sci. Technol.* **65**, 60 (2011).
- ²⁰S. Farhadi, M. Farzaneh, and S. A. Kulinich, *Appl. Surf. Sci.* **257**, 6264 (2011).
- ²¹S. A. Kulinich and M. Farzaneh, *Langmuir* **25**, 8854 (2009).
- ²²M. F. Hassan, H. P. Lee, and S. P. Lim, *Meas. Sci. Technol.* **21**, 075701 (2010).
- ²³M. Zou, S. Beckford, R. Wei, C. Ellis, G. Hatton, and M. A. Miller, *Appl. Surf. Sci.* **257**, 3786 (2011).
- ²⁴A. J. Meuler, J. D. Smith, K. K. Varanasi, J. M. Mabry, G. H. McKinley, and R. E. Cohen, *ACS Appl. Mater. Interfaces* **2**, 3100 (2010).
- ²⁵V. F. Petrenko and S. Peng, *Can. J. Phys.* **81**, 387 (2003).
- ²⁶M. He, H. Li, J. Wang, and Y. Song, *Appl. Phys. Lett.* **98**, 093118 (2011).
- ²⁷R. Karmouch and G. G. Ross, *J. Phys. Chem. C* **114**, 4063 (2010).
- ²⁸S. A. Kulinich, S. Farhadi, K. Nose, and X. W. Du, *Langmuir* **27**, 25 (2010).
- ²⁹H. H. G. Jellinek, *J. Colloid Sci.* **14**, 268 (1959).
- ³⁰See supplementary material at <http://dx.doi.org/10.1063/1.4752436> for further details of the fabrication and measurement of ice adhesion on these surfaces.